Acta Pharmaceutica Sinica B 2022;12(5):2522–2532

Chinese Pharmaceutical Association
Institute of Materia Medica, Chinese Academy of Medical Sciences

Acta Pharmaceutica Sinica B

www.elsevier.com/locate/apsb
www.sciencedirect.com

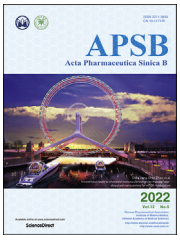

ORIGINAL ARTICLE

Inhaled curcumin mesoporous polydopamine nanoparticles against radiation pneumonitis

Ting Chen[a,b,†], Bo Zhuang[b,c,†], Yueqi Huang[b], Yan Liu[b], Bochuan Yuan[b], Wanmei Wang[b], Tianyu Yuan[b], Lina Du[a,b], Yiguang Jin[a,b,*]

[a]*Guangdong Pharmaceutical University, Guangzhou 510006, China*
[b]*Department of Pharmaceutical Sciences, Beijing Institute of Radiation Medicine, Beijing 100850, China*
[c]*Department of Chemical Defense, Institute of NBC Defense, Beijing 102205, China*

Received 12 August 2021; received in revised form 20 October 2021; accepted 22 October 2021

KEY WORDS

Radiation pneumonitis;
Curcumin;
Mesoporous;
Polydopamine;
Nanoparticle;
Pulmonary delivery;
Inhalation;
Free radical scavenging

Abstract Radiation therapy is an effective method to kill cancer cells and shrink tumors using high-energy X-ray or γ-ray. Radiation pneumonitis (RP) is one of the most serious complications of radiation therapy for thoracic cancers, commonly leading to serious respiratory distress and poor prognosis. Here, we prepared curcumin-loaded mesoporous polydopamine nanoparticles (CMPN) for prevention and treatment of RP by pulmonary delivery. Mesoporous polydopamine nanoparticles (MPDA) were successfully synthesized with an emulsion-induced interface polymerization method and curcumin was loaded in MPDA *via* π–π stacking and hydrogen bonding interaction. MPDA owned the uniform spherical morphology with numerous mesopores that disappeared after loading curcumin. More than 80% curcumin released from CMPN in 6 h and mesopores recovered. CMPN remarkably protected BEAS-2B cells from γ-ray radiation injury by inhibiting apoptosis. RP rat models were established after a single dose of 15 Gy ^{60}Co γ-ray radiation was performed on the chest area. Effective therapy of RP was achieved by intratracheal administration of CMPN due to free radical scavenging and anti-oxidation ability, and reduced proinflammatory cytokines, high superoxide dismutase, decreased malondialdehyde, and alleviated lung tissue damages were observed. Inhaled CMPN paves a new avenue for the treatment of RP.

*Corresponding author.
E-mail address: jinyg@sina.com (Yiguang Jin).
†These authors made equal contributions to this work.

Peer review under responsibility of Chinese Pharmaceutical Association and Institute of Materia Medica, Chinese Academy of Medical Sciences

https://doi.org/10.1016/j.apsb.2021.10.027

1. Introduction

Radiation pneumonitis (RP) is a typical inflammation of the lung following the stereotactic body radiotherapy for thoracic cancers, including lung cancer, breast cancer, esophageal cancer, thymic tumors, mesothelioma, lymphomas, and other malignant tumors on the chest[1−3]. RP usually develops in the first few weeks to months from initiation of radiotherapy and shows symptomatic changes such as cough, shortness of breath, and fever, with or without changes in pulmonary function tests[2,4]. RP affects 15%−40% of people who undergo radiotherapy for lung cancer and these patients have to be tormented by RP besides cancer[5−7]. RP is likely to take severe respiratory problems, such as acute respiratory distress syndrome (ARDS) that is a potentially life-threatening condition[4,8]. Moreover, it would develop to radiation pulmonary fibrosis in the late stage, even leading to respiratory failure[9,10]. Currently, the clinical treatment of RP aims to decrease inflammation using high-dose of corticosteroids; however, the side effects are obvious, such as weight gain, hyperglycemia, sleep disturbances, mood changes, and edema, so that corticosteroids are not suitable for the prevention of RP or long-term application[11,12]. Therefore, a safe and effective treatment of RP is urgently needed.

Radiation injury is related to the production of reactive oxygen species (ROS), oxidative stress, and the secretion of proinflammatory cytokines[13]. Curcumin, a polyphenolic compound, mainly extracted from the rhizome of turmeric, is reported to alleviate radiation injury by anti-inflammation, anti-oxidation, and free radical scavenging[14]. It would become a non-hormonal anti-inflammatory candidate for the treatment of RP[15]. However, the clinical application of curcumin is limited for its poor water solubility, instability, low bioavailability, and rapid clearance in the body[16]. Many efforts have been tried to overcome these problems, such as local delivery of curcumin and nanoparticle formulations[17−20]. Local administration of curcumin may be a fundamental solution to its biomedical application because it takes effects in regional area. Although nanoparticle formulations could increase the water dispersing capability and bioavailability of curcumin, the drug loading efficiency and the biocompatibility of vehicles are still challenges[21,22].

Polydopamine (PDA) is a bioinspired fascinating polymer with multiple interesting features including the simple preparation protocol, biocompatibility, free radical scavenging[23−25], and photothermal/photoacoustic properties[26]. Moreover, the free radical scavenging ability of PDA makes it be a suitable candidate for prevention of RP, which has been applied for therapy of inflammations[27,28]. PDA could be degraded into its monomers and oligomers but no obvious pharmacological effect of dopamine, exhibiting excellent biosafety[29]. Another advantage of PDA is that it owns the strong molecular adsorption capacity for bioactive chemicals. More importantly, PDA can be easily prepared to mesoporous nanoparticles that are suitable for pulmonary delivery due to high lung deposition[28,30]. Porous carriers can deliver high doses of drugs depositing in the lung after inhalation and they provide the opportunity of drug controlled release in the lung[31].

Pulmonary drug delivery is an attractive noninvasive method by inhalation. Inhalation is commonly regarded as the most efficient treatment strategy for lung diseases such as asthma, pneumonia, chronic obstructive pulmonary disease (COPD) and lung cancer due to direct high-dose drug delivery into the lung[19,32−34]. Dry powder inhalers (DPIs) are portable solid powder delivery units[35,36]. The stability of loaded drugs is usually better in DPIs than in aerosols and nebulizers. DPIs offer good patient convenience and compliance. Therefore, the inhalation of curcumin powder formulations may become an ideal strategy for the prevention of RP.

Here, curcumin-loaded mesoporous PDA nanoparticles (CMPN) were prepared and intratracheally (i.t.) administered to the lung for prevention and treatment of RP (Fig. 1). To our knowledge, this is the first report of pulmonary delivery of curcumin and polydopamine formulations for the prevention and treatment of RP. CMPN can be directly delivered to target the lung tissue by inhalation, enhancing the treatment efficiency of RP by the free radical scavenging and anti-oxidation effect of both drugs and carriers. The characteristics of CMPN were thoroughly investigated and the high therapeutic efficiency and the mechanism were evidenced by the pharmacological study.

2. Materials and methods

2.1. Materials

Curcumin and 1,3,5-trimethylbenzene (TMB) were purchased from Beijing InnoChem Science &Technology Co., Ltd., Beijing, China.

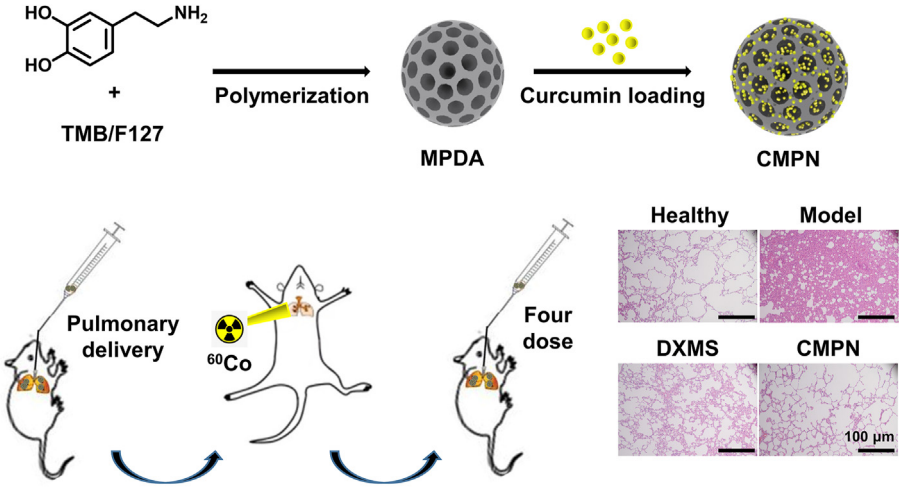

Figure 1 Schematic illustration of inhaled curcumin-loaded mesoporous polydopamine nanoparticles (CMPN) against radiation pneumonitis.

Dopamine hydrochloride was obtained from Shanghai Aladdin Bio-Chem Technology Co., Ltd., Shanghai, China. Pluronic F127 was purchased from Shandong Yousuo Chemical Technology Co., Ltd., Linyi, China. 1,1-Diphenyl-2-trinitrophenylhydrazine (DPPH) was purchased from Tokyo Chemical Industry, Tokyo, Japan. Dexamethasone (DXMS) was from Tianjin King York Pharmaceutical Co., Ltd., Tianjin, China. HLC-8 media were from Gibco, Grand Island, NY, USA. ELISA kits for rat TNF-α, IL-6, IL-1β and TGF-β1 were obtained from Beijing Neobioscience Technology Co., Ltd., Beijing, China. Purified water was prepared using Heal Force Super NW Water System (Shanghai Canrex Analytic Instrument Co., Ltd., Shanghai, China). All other reagents were of analytical grade without further purification.

2.2. Cells and animals

A normal bronchial epithelium cell line (BEAS-2B) was obtained from the Cell Bank of the Chinese Academy of Sciences (Shanghai, China). Male Sprague−Dawley rats (170−180 g) were provided by the Beijing Vital River Laboratory Animal Technology Co., Ltd., Beijing, China. All experimental procedures were executed according to the protocols approved by the Ethical Committee of Academy of Military Medical Sciences.

2.3. Synthesis of mesoporous polydopamine nanoparticles

Mesoporous polydopamine (PDA) nanoparticles (MPDA) were prepared by emulsion-induced interface polymerization[37,38]. Firstly, Pluronic F127 (0.5 g) and TMB (0.8 mL) were added into the mixed solvent (water/ethanol, 1:1, *v*/*v*, 50 mL). The mixture was magnetically stirred for 30 min to form a white emulsion followed by addition of ammonia (1.875 mL) and dopamine hydrochloride (0.75 g) and then the reaction was continued for 2 h at room temperature. The suspension was centrifuged for 10 min at 14,800×*g* (H2-16KR, Hunan Kecheng Instrument Equipment Co., Ltd., Changsha, China). The precipitates were collected and washed with water/ethanol (1:1, *v*/*v*) twice and the emulsion templates were removed with ethanol/acetone (2:1, *v*/*v*) under sonication (30 min, three times). The precipitates were dried at 40 °C for 4 h to obtain black MPDA powders.

2.4. Preparation and characterization of CMPN

Curcumin (100 mg) was dissolved in ethanol (100 mL) and MPDA (100 mg) was added. The mixture was stirred overnight at room temperature and then dried under vacuum to obtain the powders of curcumin mesoporous polydopamine nanoparticles (CMPN). Curcumin was analyzed with a high-performance liquid chromatography (HPLC, Agilent 1260, USA) as the following conditions: a Diamonsil C18 ODS column (250 mm × 4.6 mm, 5 μm), a mobile phase of acetonitrile/water/acetic acid (50:49:1, *v*/*v*/*v*) at a flow rate of 1 mL/min, an injection volume of 20 μL, the detection wavelength of 425 nm, and the column temperature at 30 °C. For the determination of drug loading efficiency, CMPN was thoroughly dispersed in ethanol under ultrasound and centrifuged (14,800×*g*, 10 min) to separate curcumin, and then the supernatant was filtered for curcumin determination using HPLC. The drug loading efficiency was calculated according to formula as shown in Eq. (1).

$$\text{Loading efficiency (\%)} = \text{Total curcumin/Total CMPN} \times 100 \quad (1)$$

The particle sizes and zeta potentials of CMPN were measured with the dynamic light scattering (DLS) method on Zetasizer Nano ZS (Malvern, UK) at 25 °C. The morphology of CMPN was inspected using a transmission electron microscope (TEM, H-7650, Hitachi, Tokyo, Japan) after staining with 2% sodium phosphotungstate solutions. The surface structures of MPDA and CMPN were observed under a scanning electron microscope (SEM, S-4800, Hitachi, Tokyo, Japan). In addition, the simulated lung deposition of CMPN powders was measured at 60 L/min using the next generation impactor (NGI, TPK 2000R, Copley, British). The deposited powders in every stage were collected and curcumin was separately determined as above. The fine particle fraction (FPF) of CMPN powders was calculated after the drug contents in Stages 3−7 were divided by the contents in the whole system. The FPF and mass median aerodynamic diameter (MMAD) of CMPN were calculated using the CITDAS software (Version 3.10 Wibu USP32/Ph. Eur. 6.0, the COPLEY company, Nottingham, UK).

The interaction of curcumin and CMPN was identified with the Fourier Transform Infrared spectrometry (FTIR, Spectrum Two, PerkinElmer, USA). An X-ray diffraction (XRD) method was used to investigate the crystalline phase of curcumin in CMPN with the Ni filtered Cu Kα radiation and the XRD instrument (Rigaku Ultiam IV, Japan).

2.5. In vitro drug release study

CMPN (containing *ca.* 1 mg curcumin) was added to a triangular flask and suspended in 50 mL of the simulated lung fluid containing 0.05% Tween 80[39]. The flask was placed on a shaker (100 rpm, THZ-D, Taicang Laboratory Instrument Factory, Suzhou, China) at 37 °C for *in vitro* drug release investigation. At the predetermined time points (0.25, 0.5, 1, 2, 4, 6, 8 and 12 h), an aliquot (1 mL) of the media was withdrawn and replaced with the fresh media of equal volume. The sample was centrifuged at 14,800×*g* for 10 min to exclude the nanoparticles. The supernatant was filtered through a 0.22-μm filter and analyzed with HPLC to determine released curcumin. Additionally, the morphological changes of CMPN were observed with SEM at different release time points. The experiments were performed in triplicates.

2.6. Assay of free radical scavenging ability

The free radical scavenging ability of MPDA and curcumin were tested using the DPPH method[40]. Briefly, an ethanol solution of DPPH (0.05 mg/mL) was prepared in the dark. MPDA (3 mg) or curcumin (1 mg) was added to the ethanol solution (1 mL). After incubation for 30 min in the dark, the MPDA-contained solution was centrifuged (14,800×*g*, 10 min) to separate the particles. The supernatant was tested with an electron spin resonance (ESR) spectrometer (Bruker-A300, Karlsruhe, Germany). The curcumin-contained solution was directly tested without centrifugation. The ESR spectra were recorded with the following conditions: microwave power, 1 mW; modulation amplitude, 1 G; sweep field width, 300 G; sweep time, 180 s. The ethanol solution of DPPH was used as the control.

2.7. Investigation of CMPN cytotoxicity

The cytotoxicities of curcumin and CMPN were investigated on BEAS-2B cells using Cell Counting Kit-8 (CCK-8, Gen-View Sciences Inc., USA). The BEAS-2B cells were seeded in 96-well

plates at a density of 10^4 cells/well and incubated for adherence. Curcumin and CMPN were dissolved or dispersed in dimethyl sulphoxide (DMSO), respectively, and then diluted with the culture media to a series of concentrations. The doped culture media were added to the plates where the final DMSO concentration kept less than 0.1%. The cells were incubated for 24 h and the cell viability was calculated according to the absorbance of cells after 2 h incubation with 10% CCK-8 regents. The absorbance at 450 nm was detected using a microplate reader (ELX800, BioTek Instrument, USA).

2.8. Analysis of BEAS-2B cell apoptosis after irradiation

BEAS-2B cells were seeded in 6-well plates at a density of 2×10^5 cells/well and incubated for 24 h. The cells were treated with curcumin or CMPN and the final concentration of curcumin was maintained at 31.25 μmol/L. After incubation for 24 h, the BEAS-2B cells were irradiated with 15 Gy ^{60}Co γ-ray (Beijing Institute of Radiation Medicine). Twenty-four hours later, cell apoptosis was detected with a flow cytometer (BD II, BD Biosciences, Franklin Lakes, NJ, USA) after V-FITC/PI staining.

2.9. Pharmacodynamic study

Twenty rats were randomly divided into 4 groups: the healthy group (no irradiation), the model group (irradiation without treatment), the DXMS group (irradiation with i.t. dexamethasone), and the CMPN group (irradiation with i.t. CMPN). Irradiation was performed on the area of rat chest with a single dose of 15 Gy ^{60}Co γ-ray at a dose rate of 98.16 cGy/min. DXMS (2.5 mg/kg) or CMPN (containing 2 mg curcumin) was i.t. administered to the rats 5 h pre-irradiation and once a week for consecutive 4 weeks post-irradiation. The CMPN was i.t. administered at 5 h pre-irradiation for consideration of drug release (Fig. 2G). The time period of 5 h would be sufficient to get ready for clinical thoracic radiotherapy. Before the i.t. administration of DXMS or CMPN, the rats were anesthetized with isoflurane using a gas anesthesia system (Shanghai Yuyan Instruments Co., Ltd., Shanghai, China), and then we sprayed the drug formulations into the lung through the trachea with an insufflator (Model DP-4, Penn-Century, Inc., USA). During the experimental period, the rat living states were carefully observed and the body weight was recorded. In addition, the complete blood counting was performed for investigation of the hematopoietic system injury caused by radiation. On Days −1, 1, 3, 6, 10, 14, 21 and 28, an aliquot (20 μL) of tail vein blood was collected and mixed with the diluent (2 mL) for analysis, respectively. The white blood cells (WBC), platelets (PLT), red blood cells (RBC) and neutrophils (NE) in the blood were counted with a CelltacE automatic blood cell analyzer (MEK-7222k, Nihon Kohden, Japan).

2.10. Histopathological examination

The rats were sacrificed at the end of the pharmacodynamic study and the whole lung tissues were excised. The upper lobe of the right lung was immersed in 10% formalin solutions for 24 h and then embedded in paraffin. After hematoxylin and eosin (H&E) and Masson staining, the pathological sections were observed under a microscope (BDS200-FL, Chongqing Optec Instrument Co., Ltd., Chongqing, China).

2.11. ELISA measurement

The middle lobes of the right lung of rats were homogenized with a homogenizer (KI-II, Servicebio, Wuhan, China) at 60 Hz for 4 min, and then centrifuged at 14,800×g for 20 min. The supernatants were collected for detection of TNF-α, IL-6, IL-1β and TGF-β1 with ELISA kits according to the manufacturer's instructions. The levels of superoxide dismutase (SOD), malondialdehyde (MDA) and total proteins in the lung homogenates were also detected with ELISA kits.

2.12. Statistical analysis

All data were expressed as mean ± standard deviation (SD). The results were calculated statistically using the SPSS 19.0 software (SPSS, Chicago, IL, USA). One-way analysis of variance (ANOVA) with the LSD test was used to identify differences ($P < 0.05$ or $P < 0.01$) between the data.

3. Results and discussion

3.1. Characteristics of CMPN

MPDA was successfully prepared by dopamine polymerization on the interface of the emulsion templates. TMB acted as the organic phase core to form the emulsion. Thanks to the π-electron rich structure of TMB, dopamine self-assembled on the surface of the emulsion based on the π−π stacking interaction and polymerized to PDA under the alkaline circumstance. After removal of TMB and pluronic-F127, the mesoporous structure, *i.e.*, MPDA, was obtained. We verified the chemical structure of MPDA with FTIR, exhibiting obvious signals of stretching vibration of C−C, C−N and the indole ring (Supporting Information Fig. S1). CMPN was further obtained after curcumin was loaded in MPDA mainly based on π–π stacking and hydrogen bonding interactions. Interestingly, MPDA was black solid powders (Fig. 2A), while CMPN was yellowish-brown due to the doping of a large amount of curcumin (Fig. 2B). Moreover, many mesopores appeared on the surface of spherical MPDA (Fig. 2C), but the mesopores disappeared in CMPN, which should be attributed to the filling of mesopores with curcumin (Fig. 2D). Thanks to the mesoporous structure and high specific surface area of MPDA, the curcumin loading efficiency was high to about 47%. In recent years, mesoporous materials, characterized with the unique pore size, high surface area and pore volume, are widely explored as drug carriers. The large inner space and many surface pores of mesoporous materials provide the basis of great drug entrapment and adsorption, leading to high drug loading efficiency. The TEM image further revealed that CMPN were uniform spheres (inserted picture in Fig. 2E). The average particle size of CMPN was 290.73 ± 29.73 nm ($n = 3$) with uniform size distribution (PDI = 0.216 ± 0.017, $n = 3$) and the zeta potential was −26.4 ± 3.1 mV ($n = 3$, Fig. 2E and F). The zeta potential value of about −30 mV is considered optimum for nanoparticle stability[41].

The release of water-insoluble drugs is a key factor for clinical applications[42]. Curcumin release from CMPN was relatively stable and rapid with more than 80% accumulative release within 6 h (Fig. 2G), which would improve the biological protection from irradiation. Interestingly, we found that the surface mesopores of

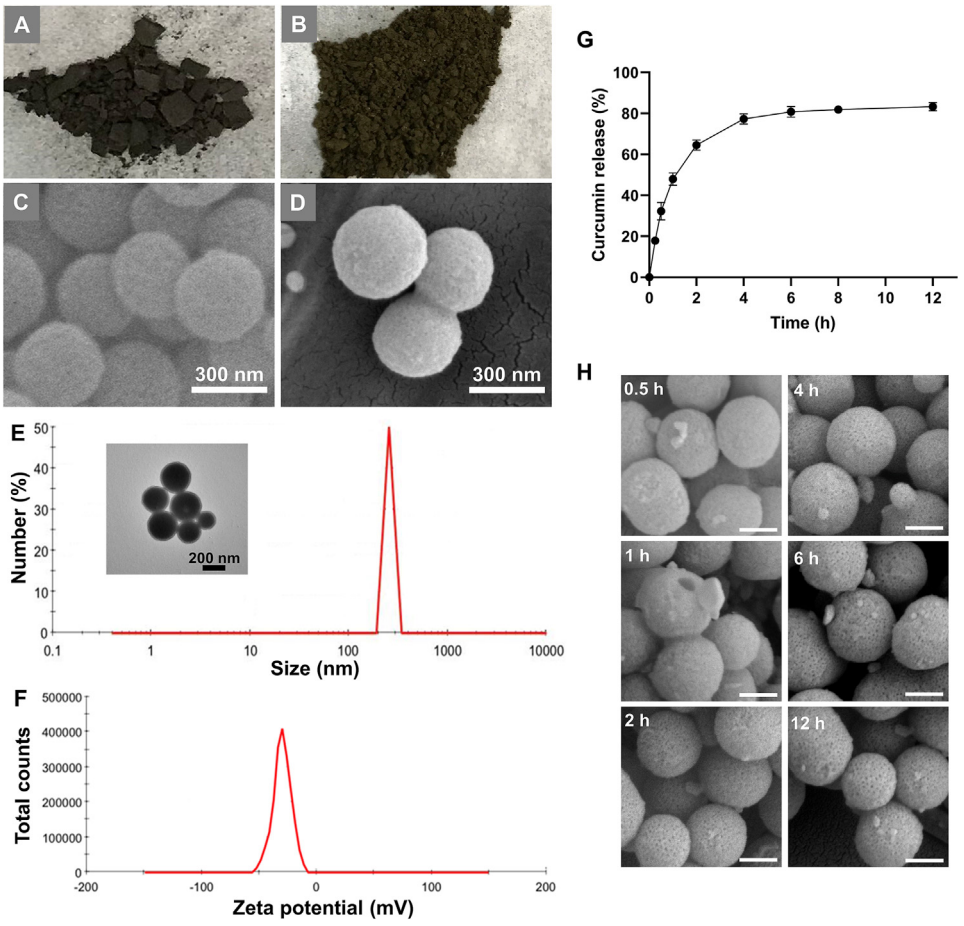

Figure 2 Characteristics of CMPN. Appearance of MPDA powders (A) and CMPN powders (B). SEM images of MPDA (C) and CMPN (D). (E) Size distribution of CMPN (the inserted picture was the TEM image of CMPN). (F) Zeta potential of CMPN. (G) Release profile of curcumin from CMPN, the data are presented as mean ± SD (n = 3). (H) SEM images of residual CMPN after release for different time, Scale bar = 200 nm.

the particles gradually reappeared with curcumin release by SEM observation of residual CMPN particles (Fig. 2H).

The water solubility of curcumin is often influenced by its state, which would likely affect its release behavior, also *in vivo* pharmacological effect[42,43]. In this study, the state of curcumin in CMPN was identified by multiple methods. The FTIR spectra of curcumin showed a characteristic peak of phenolic hydroxyl stretching vibration at 3508 cm^{-1} (Fig. 3A). The physical mixture of MPDA/curcumin also showed the specific peak of phenolic hydroxyl while the specific peak disappeared in CMPN, which might be attributed to the hydrogen bonding between curcumin and MPDA. Additionally, the XRD spectra showed that MPDA was amorphous, while curcumin had a crystalline structure. The crystalline peak of curcumin still existed in the physical mixture

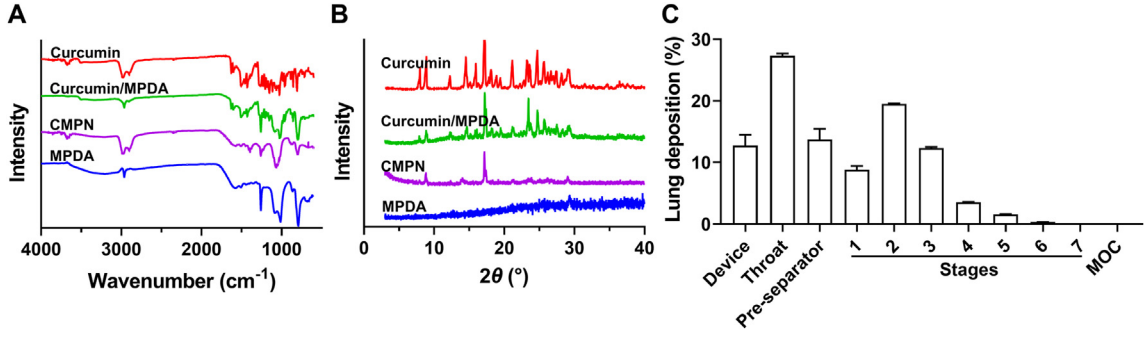

Figure 3 State of curcumin in CMPN and the simulated drug lung deposition. FTIR spectra (A) and XRD spectra (B) of curcumin, the physical mixture of curcumin/MPDA, CMPN, and MPDA. (C) Simulated drug lung deposition of CMPN powders. Data are presented as mean ± SD (n = 3).

but almost disappeared in CMPN (Fig. 3B). The difference between the mixture and CMPN indicated that the crystalline curcumin in CMPN was little. Amorphous powder inhalers offer the benefits of increased *in vivo* pharmacological effect for poorly soluble drugs[44].

Effective lung deposition is one of the key elements for inhalation drug formulation. The FPF of inhaled powders is an important parameter for evaluation of lung deposition. The *in vitro* simulated experiment indicated the FPF of CMPN powders was 29.83 ± 0.24%, and the MMAD was 5.17 ± 0.04 μm, indicating that CMPN was appropriate for pulmonary delivery (Fig. 3C). Generally, the droplets or particles of 1−5 μm in aerodynamic diameter are likely to deposit in the small airways and alveoli and more than 50% of the 3 μm diameter particles deposit in the alveolar region[33,45]. The DLS size of CMPN was several hundred nanometers. So did the electron microscopic size of them. However, PDA usually exhibits adhesive property[46], leading to CMPN assembling to microparticles (Fig. 2D and E). The aggregated CMPN powders had suitable MMAD (5.17 μm) for lung deposition. Therefore, CMPN can be inhaled in dry powders. Moreover, porous nanoparticle-aggregate-based particles are recognized as one of the most promising carriers for controlled drug release in the lung[31]. The mesoporous particles possess the smaller aerodynamic particle size compared to the solid particle with the same size, leading to more lung deposition and avoiding the phagocytosis of alveolar macrophages[32].

3.2. *Strong free radical scavenging ability of MPDA and curcumin*

DPPH assay is often used to measure the free radical scavenging ability of compounds, where the reaction can maintain stable for hours in solutions[40]. Both MPDA and curcumin turned the color of DPPH solutions to light yellow from pink. Moreover, the ESR peaks of DPPH disappeared after incubation with MPDA and curcumin, indicating that the free radicals were scavenged (Fig. 4). The strong free radical scavenging ability of MPDA and curcumin would benefit CMPN scavenging the free radicals in the lung tissues after γ-ray irradiation and alleviating radiation injury.

3.3. *High safety and radiation protection effect of CMPN on BEAS-2B cells*

BEAS-2B cells are normal bronchial epithelium cells, which are commonly used as the subjects of inhalation toxicity investigation. Curcumin showed high safety with no cytotoxicity on BEAS-2B cells even at a high concentration of 125 μmol/L (Fig. 5A). The effect of CMPN on BEAS-2B cells was very similar to that of curcumin, indicating the high safety of CMPN (Fig. 5A). Moreover, the *in vivo* safety of inhaled curcumin had been already confirmed by the previous reports[47,48]. Inhaled curcumin is safe in animals even when the animals are exposed to the material over long periods. Therefore, CMPN should be safe when inhalation to the lung.

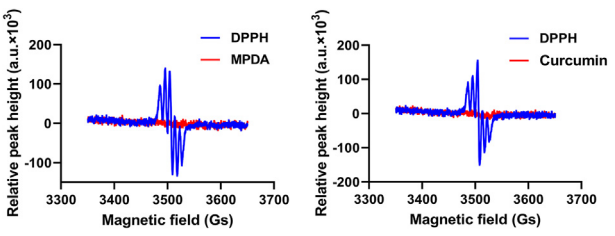

Figure 4 ESR spectra of DPPH after incubation with MPDA and curcumin.

The aim of radiation therapy is to induce cancer cell apoptosis and death; however, it simultaneously leads to unwanted injury on normal cells[49]. In this study, BEAS-2B cells were used to explore the protection effect of CMPN. The flow cytometric results remarkably showed the radiation protection effect of curcumin and CMPN with the apoptosis rates of 19.1% and 13.45%, respectively, compared to the high apoptosis rate (>30%) of the control cells after γ-ray irradiation (Fig. 5B). The higher protection effect of CMPN than curcumin could be attributed to the stronger free radical scavenging and anti-oxidation ability of CMPN that rapidly released curcumin to the surroundings. Besides the rapid curcumin release from CMPN, another advantage of CMPN could be enhanced mucus penetration and cell uptake. Recent studies have verified the superior mucus penetrating ability and cell uptake of PDA-modified nanoparticles[50,51].

3.4. *Protection of hematopoietic system by CMPN*

The hematopoietic system is extremely sensitive to ionizing radiation with remarkable decrease of bone marrow cells (BMC) and circulating peripheral blood cells[52]. Therefore, the counting of blood cells is an important method to evaluate ionizing radiation-induced injury and the protection and treatment efficiency of medicines. All the radiation-exposed rats showed the sharp decrease of WBC compared to the heathy ones, especially in the model group (Fig. 6A). Their WBC began to recover on Day 7, where DXMS and CMPN improved the recovery. The WBC in the CMPN group was significantly higher than that in the model group at some time points, such as Days 1, 14, and 28 ($P < 0.05$), but there was no significant difference between the CMPN and DXMS groups. PLT exhibited the similar profiles to WBC and no significant difference was shown between the CMPN and DXMS groups too (Fig. 6B). Therefore, the pulmonary delivery of DXMS and CMPN alleviated the hematopoietic damage induced by chest ionizing radiation to some extent. However, RBC and NE did not show significant difference between all groups (Fig. 6C and D), indicating that local ionizing radiation may not hurt the hematopoietic system as seriously as the systemic radiation[53,54]. The radiation injury is also highly related to the radiation dose. Clinical radiation therapy commonly applies 45−60 Gy for the treatment of breast, head, and neck cancers, although the doses are divided into multiple smaller doses. In the preclinical studies of RP, the radiation conditions are different, although 15 Gy ^{60}Co γ-ray radiation was usually used for establishment of RP animal models[16,55]. In the preliminary study, we had screened the radiation dose for establishment of RP rat models, involving 10, 15, and 20 Gy. Finally, we found that the dose of 15 Gy was suitable for establishment of moderate RP with little systemic damage.

The body weight of irradiated rats decreased until Day 7 and then recovered with the increasing profiles (Fig. 6E), where the DXMS and CMPN groups recovered faster than the model group. Moreover, the CMPN group maintained the highest body weight among the three irradiation groups, indicating the best prevention and treatment of irradiation injury. The living state of rats represents their whole health states. The rats in the model group exhibited obvious dispiritedness, anorexia, piloerection, and delayed

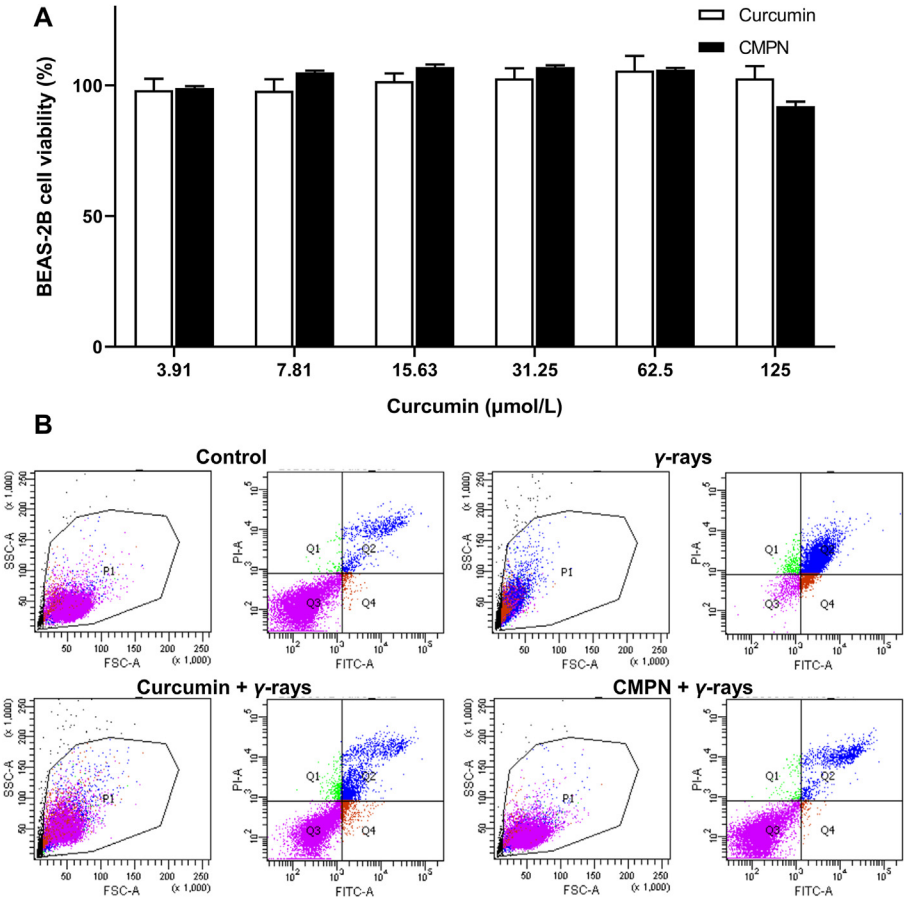

Figure 5 High safety and radiation protection effect of CMPN on BEAS-2B cells. (A) Cell viability of BEAS-2B cells after incubation with curcumin and CMPN. (B) Flow cytometry plots of BEAS-2B cells after FITC/PI staining. Data are presented as mean ± SD ($n = 5$).

reactions, while DXMS and CMPN alleviated the above adverse states. Additionally, the mental state of the rats in the CMPN group was better than that in the DXMS group and the formers showed significant activity, normal breathing, and smooth fur.

3.5. *Highly effective anti-lung injury effect of CMPN*

Ionizing radiation seriously damages the lung tissues, leading to RP[10]. The lung tissues of RP showed obvious hemorrhages,

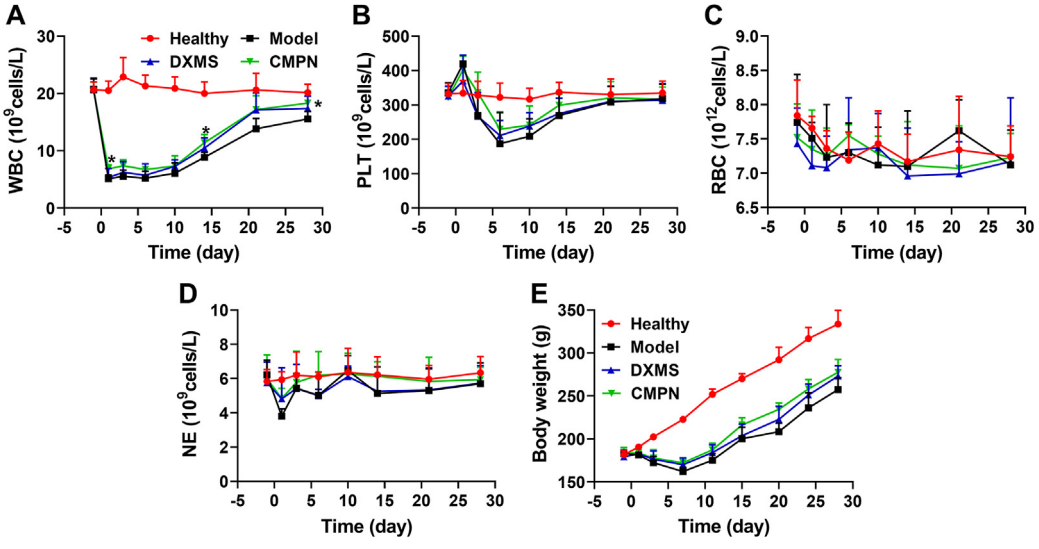

Figure 6 Cell counts in the peripheral blood and the body weight of rats. WBC (A), PLT (B), RBC (C), and NE (D) in the peripheral blood. (E) Body weight profiles of rats. The data are presented as mean ± SD ($n = 5$). *$P < 0.05$ between the CMPN and Model groups.

sporadic white nodules, and diffuse alveolar congestion, more importantly, remarkable pulmonary fibrosis, compared to the ruddy and smooth appearance and the clear normal lung alveolar septum and well distributed alveolar walls of the healthy lung tissues (Fig. 7). Radiation-induced pulmonary fibrosis is an emerging disease, which destructs the lung tissue progressively and irreversibly. Both DXMS and CMPN significantly alleviated the hemorrhaging and pulmonary fibrosis in the lung tissues compared to the model group, although a little fibrosis was still present. The CMPN group seemed better than the DXMS group with no hemorrhaging, little infiltrating inflammatory cells and the clear alveolar structure. All the irradiated groups showed enlarged lung tissues compared to the healthy group, probably resulting from the thickened texture and edema. Therefore, CMPN is an effective medicine for prevention of pulmonary fibrosis induced by irradiation.

3.6. *High anti-inflammation effect of CMPN*

Cytokines are the regulators of host immune responses to infection, inflammation, and trauma. Some cytokines (*e.g.*, TNF-α, IL-6, IL-1β, and TGF-β1) play key roles in the inflammation development process[56]. TNF-α is an important proinflammatory cytokine in early radiation lung injury, which represents the extent of lung injury[57]. IL-6, IL-1β, and TGF-β1 are also closely related to the occurrence and development of RP. Moreover, TGF-β1 directly acts on the later stage of RP, promoting the development of radiation fibrosis[58]. TNF-α, IL-6, IL-1β and TGF-β1 in the model group significantly increased compared to the healthy one ($P < 0.01$, $P < 0.001$, $P < 0.05$, $P < 0.01$, respectively, Fig. 8), indicating that radiation induced the occurrence of pneumonia. By contrast, the inflammatory cytokines decreased remarkably after treatment with DXMS or CMPN, even close to the normal levels (Fig. 9). Therefore, both of CMPN and DXMS had strong anti-inflammatory effects to alleviate the lung injury induced by irradiation.

3.7. *High anti-oxidation effect of CMPN*

SOD is found to be predominantly and highly expressed in the extracellular matrix of lung and helps to break down potentially harmful oxygen molecules[59]. Due to its strong oxygen radical scavenging ability, SOD can reduce acute radiation toxicity caused by over-oxidation[60]. MDA is one of the main lipid peroxides, which can trigger a chain reaction of radicals[61]. Additionally, the alveolar epithelial cell damage would lead to an increase of total protein content in the lung homogenate[62]. In this study, the SOD in the model group decreased sharply compared to that in the healthy group ($P < 0.01$, Fig. 9A), because it was greatly consumed by the irradiation-induced oxygen radicals. Meanwhile, the MDA and total proteins in the model group increased remarkably (Fig. 9B and C), indicating the lipid peroxidation reaction and alveolar epithelial cell damage. By contrast, after treatment with DXMS or CMPN, SOD increased while MDA and total proteins decreased, indicating their effectiveness against RP. Moreover, CMPN exhibited better therapeutic effect on RP than DXMS in term of total proteins in the lung tissues, although no statistical difference of SOD and MDA was shown between them. Therefore, CMPN improved SOD activity for anti-oxidation, inhibited lipid peroxidation, and protected alveolar epithelial cells, favoring the treatment of RP.

Here, we demonstrate that both of CMPN and DXMS had significant therapeutic efficiency for RP, involving reduced proinflammatory cytokines, high SOD, decreased MDA and total proteins, and alleviated lung tissue damage. However, the therapeutic effect of CMPN was better than that of DXMS in some aspects, such as lower total proteins in the lung tissues, prevention

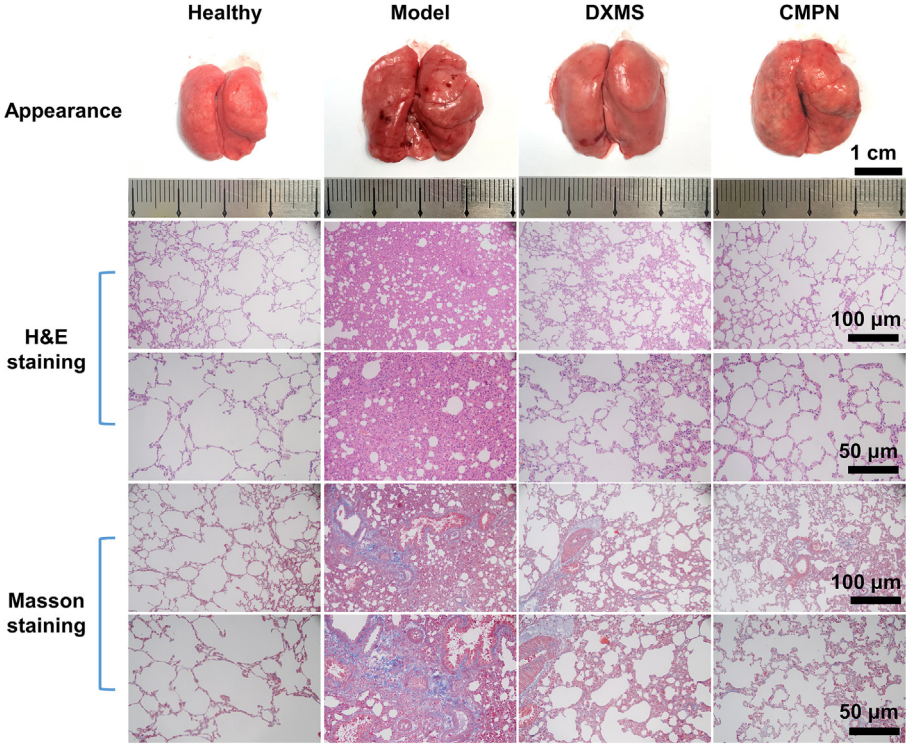

Figure 7 Appearance, H&E staining and Masson staining of lung tissues.

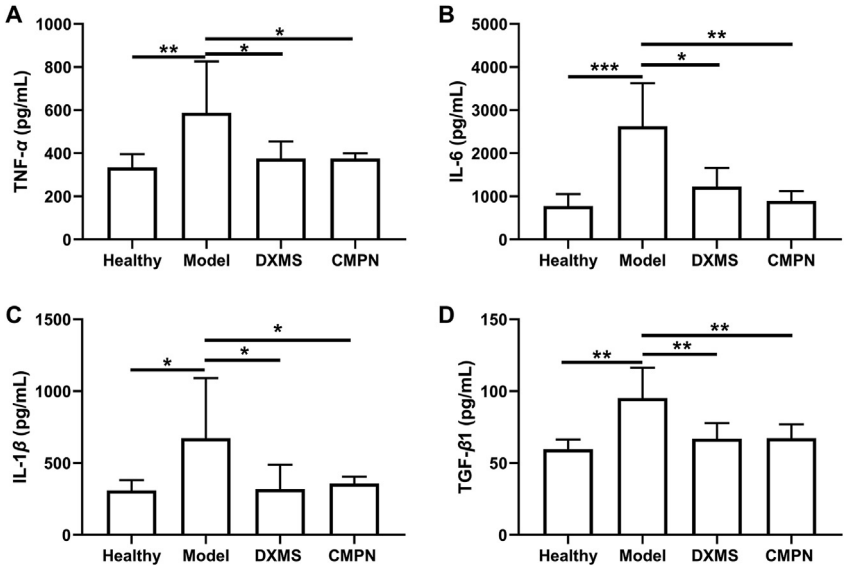

Figure 8 Cytokines in the lung tissues. (A) TNF-α, (B) IL-6, (C) IL-1β, and (D) TGF-β1 in the lung tissues. Data are presented as mean ± SD ($n = 4$). *$P < 0.05$, **$P < 0.01$, ***$P < 0.001$.

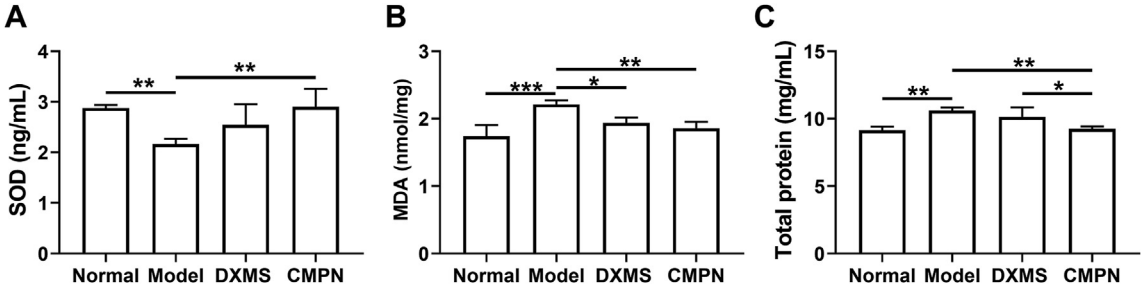

Figure 9 Levels of SOD (A), MDA (B) and total proteins (C) in the rat lung tissues. Data are presented as mean ± SD ($n = 3$). *$P < 0.05$, **$P < 0.01$, ***$P < 0.001$.

of pulmonary fibrosis, and alleviated lung tissue damage. Glucocorticoids are widely used for therapy of pneumonitis, achieving positive clinical outcome to some extent[63]. However, the side effects of glucocorticoids are obvious, such as body weight gain, hyperglycemia, sleep disturbances, mood changes and edema, indicating that these medicines are not suitable for prevention of RP or long-term application[12]. Moreover, glucocorticoids have inhibitory effects on a broad range of immune responses, leading to immunosuppressive effect. Consistently, glucocorticoids strongly suppress cell-mediated immunity and cause viral infection and tumor development[64,65]. Therefore, inhaled CMPN becomes a promising alternative strategy for prevention or treatment of RP due to its safety and high effectiveness.

4. Conclusions

RP is one type of severe common clinical diseases but effective and safe treatments are absent. In this study, curcumin and PDA were proved to have great anti-oxidation and free radical scavenging ability, suitable as the active drug and carrier for prevention and treatment of RP. The mesoporous structure of MPDA provided the large inner space and numerous surface pores to obtain high drug loading efficiency. Moreover, the amorphous state of curcumin in CMPN improved its dissolution and release to make the prevention and treatment very quickly after pulmonary delivery. Besides the anti-oxidation and free radical scavenging ability, inhaled CMPN guaranteed the highly effective prevention and treatment of RP by reduced proinflammatory cytokines, enhanced SOD, decreased MDA, and alleviated lung tissue damage. The combination of curcumin and MPDA and the unique administration route, *i.e.*, inhalation of CMPN, are the keys to the prevention and treatment of RP.

Acknowledgments

This study is partially supported by the National Key New Drug Creation and Manufacturing Program, Ministry of Science and Technology (CN) (No. 2018ZX09J18104-001).

Author contributions

Ting Chen, Bo Zhuang and Yiguang Jin designed the research, carried out the experiments and performed data analysis. Yueqi Huang, Yan Liu, Wanmei Wang, and Tianyu Yuan participated part of the experiments. Bochuan Yuan, Lina Du and Yiguang Jin supervised the experiments and performed data analysis. Ting

Chen, Bo Zhuang and Yiguang Jin wrote and revised the manuscript. All authors have read and approved the final manuscript.

Conflicts of interest

The authors have no conflicts of interest to declare.

Appendix A. Supporting information

Supporting data to this article can be found online at https://doi.org/10.1016/j.apsb.2021.10.027.

References

1. Bledsoe TJ, Nath SK, Decker RH. Radiation pneumonitis. *Clin Chest Med* 2017;**38**:201−8.
2. Hanania AN, Mainwaring W, Ghebre YT, Hanania NA, Ludwig M. Radiation-induced lung injury: assessment and management. *Chest* 2019;**156**:150−62.
3. Aso S, Navarro-Martin A, Castillo R, Padrones S, Castillo E, Montes A, et al. Severity of radiation pneumonitis, from clinical, dosimetric and biological features: a pilot study. *Radiat Oncol* 2020;**15**:246.
4. Arroyo-Hernández M, Maldonado F, Lozano-Ruiz F, Muñoz-Montaño W, Nuñez-Baez M, Arrieta O. Radiation-induced lung injury: current evidence. *BMC Pulm Med* 2021;**21**:9.
5. Jain V, Berman AT. Radiation pneumonitis: old problem, new tricks. *Cancers (Basel)* 2018;**10**:222.
6. Ullah T, Patel H, Pena GM, Shah R, Fein AM. A contemporary review of radiation pneumonitis. *Curr Opin Pulm Med* 2020;**26**:321−5.
7. Palma DA, Senan S, Tsujino K, Barriger RB, Rengan R, Moreno M, et al. Predicting radiation pneumonitis after chemoradiation therapy for lung cancer: an international individual patient data meta-analysis. *Int J Radiat Oncol Biol Phys* 2013;**85**:444−50.
8. Thomas R, Chen YH, Hatabu H, Mak RH, Nishino M. Radiographic patterns of symptomatic radiation pneumonitis in lung cancer patients: imaging predictors for clinical severity and outcome. *Lung Cancer* 2020;**145**:132−9.
9. Azmoonfar R, Amini P, Saffar H, Rezapoor S, Motevaseli E, Cheki M, et al. Metformin protects against radiation-induced pneumonitis and fibrosis and attenuates upregulation of dual oxidase genes expression. *Adv Pharm Bull* 2018;**8**:697−704.
10. Li W, Lu L, Liu B, Qin S. Effects of phycocyanin on pulmonary and gut microbiota in a radiation-induced pulmonary fibrosis model. *Biomed Pharmacother* 2020;**132**:110826.
11. Xia C, Shi W, Zhang Y, Ding L, Gao L, Wang Q, et al. Prevention and treatment of radiation-induced lung injury. *Future Med Chem* 2020;**12**:2161−73.
12. Khan NA, Donatelli CV, Tonelli AR, Wiesen J, Ribeiro Neto ML, Sahoo D, et al. Toxicity risk from glucocorticoids in sarcoidosis patients. *Respir Med* 2017;**132**:9−14.
13. Simone CB. Thoracic radiation normal tissue injury. *Semin Radiat Oncol* 2017;**27**:370−7.
14. Farhood B, Mortezaee K, Goradel NH, Khanlarkhani N, Salehi E, Nashtaei MS, et al. Curcumin as an anti-inflammatory agent: implications to radiotherapy and chemotherapy. *J Cell Physiol* 2019;**234**:5728−40.
15. Schwarz K, Dobiasch S, Nguyen L, Schilling D, Combs SE. Modification of radiosensitivity by curcumin in human pancreatic cancer cell lines. *Sci Rep* 2020;**10**:3815.
16. Amini P, Saffar H, Nourani MR, Motevaseli E, Najafi M, Taheri RA, et al. Curcumin mitigates radiation-induced lung pneumonitis and fibrosis in rats. *Int J Mol Cell Med* 2018;**7**:212−9.
17. Du L, Feng X, Xiang X, Jin Y. Wound healing effect of an *in situ* forming hydrogel loading curcumin-phospholipid complex. *Curr Drug Deliv* 2016;**13**:76−82.
18. Sun Y, Du L, Liu Y, Li X, Li M, Jin Y, et al. Transdermal delivery of the *in situ* hydrogels of curcumin and its inclusion complexes of hydroxypropyl-β-cyclodextrin for melanoma treatment. *Int J Pharm* 2014;**469**:31−9.
19. Zhang T, Chen Y, Ge Y, Hu Y, Li M, Jin Y. Inhalation treatment of primary lung cancer using liposomal curcumin dry powder inhalers. *Acta Pharm Sin B* 2018;**8**:440−8.
20. Hu Y, Li M, Zhang M, Jin Y. Inhalation treatment of idiopathic pulmonary fibrosis with curcumin large porous microparticles. *Int J Pharm* 2018;**551**:212−22.
21. Liu Y, Yang G, Jin S, Xu L, Zhao CX. Development of high-drug-loading nanoparticles. *Chempluschem* 2020;**85**:2143−57.
22. Hossen S, Hossain MK, Basher MK, Mia MNH, Rahman MT, Uddin MJ. Smart nanocarrier-based drug delivery systems for cancer therapy and toxicity studies: a review. *J Adv Res* 2019;**15**:1−18.
23. Jing Y, Deng Z, Yang X, Li L, Gao Y, Li W. Ultrathin two-dimensional polydopamine nanosheets for multiple free radical scavenging and wound healing. *Chem Commun (Camb)* 2020;**56**:10875−8.
24. Liu H, Qu X, Tan H, Song J, Lei M, Kim E, et al. Role of polydopamine's redox-activity on its pro-oxidant, radical-scavenging, and antimicrobial activities. *Acta Biomater* 2019;**88**:181−96.
25. Hu J, Yang L, Yang P, Jiang S, Liu X, Li Y. Polydopamine free radical scavengers. *Biomater Sci* 2020;**8**:4940−50.
26. Guan Q, Guo R, Huang S, Zhang F, Liu J, Wang Z, et al. Mesoporous polydopamine carrying sorafenib and SPIO nanoparticles for MRI-guided ferroptosis cancer therapy. *J Control Release* 2020;**320**:392−403.
27. Jin A, Wang Y, Lin K, Jiang L. Nanoparticles modified by polydopamine: working as "drug" carriers. *Bioact Mater* 2020;**5**:522−41.
28. Zhao H, Zeng Z, Liu L, Chen J, Zhou H, Huang L, et al. Polydopamine nanoparticles for the treatment of acute inflammation-induced injury. *Nanoscale* 2018;**10**:6981−91.
29. Chen X, Yang W, Zhang J, Zhang L, Shen H, Shi D. Alkalinity triggered the degradation of polydopamine nanoparticles. *Polym Bull* 2020;**78**:4439−52.
30. Garcia-Mouton C, Hidalgo A, Cruz A, Pérez-Gil J. The lord of the lungs: the essential role of pulmonary surfactant upon inhalation of nanoparticles. *Eur J Pharm Biopharm* 2019;**144**:230−43.
31. Liang Z, Ni R, Zhou J, Mao S. Recent advances in controlled pulmonary drug delivery. *Drug Discov Today* 2015;**20**:380−9.
32. Zhu L, Li M, Liu X, Du L, Jin Y. Inhalable oridonin-loaded poly(lactic-*co*-glycolic)acid large porous microparticles for *in situ* treatment of primary non-small cell lung cancer. *Acta Pharm Sin B* 2017;**7**:80−90.
33. Yang MY, Chan JG, Chan HK. Pulmonary drug delivery by powder aerosols. *J Control Release* 2014;**193**:228−40.
34. Kuzmov A, Minko T. Nanotechnology approaches for inhalation treatment of lung diseases. *J Control Release* 2015;**219**:500−18.
35. Debnath SK, Saisivam S, Omri A. PLGA ethionamide nanoparticles for pulmonary delivery: development and *in vivo* evaluation of dry powder inhaler. *J Pharm Biomed Anal* 2017;**145**:854−9.
36. Rudén J, Frenning G, Bramer T, Thalberg K, An J, Alderborn G. Linking carrier morphology to the powder mechanics of adhesive mixtures for dry powder inhalers *via* a blend-state model. *Int J Pharm* 2019;**561**:148−60.
37. Chen F, Xing Y, Wang Z, Zheng X, Zhang J, Cai K. Nanoscale polydopamine (PDA) meets pi−pi interactions: an interface-directed coassembly approach for mesoporous nanoparticles. *Langmuir* 2016;**32**:12119−28.
38. Wang Z, Wang L, Prabhakar N, Xing Y, Rosenholm JM, Zhang J, et al. CaP coated mesoporous polydopamine nanoparticles with responsive membrane permeation ability for combined photothermal and siRNA therapy. *Acta Biomater* 2019;**86**:416−28.
39. Radivojev S, Luschin-Ebengreuth G, Pinto JT, Laggner P, Cavecchi A, Cesari N, et al. Impact of simulated lung fluid components on the solubility of inhaled drugs and predicted *in vivo* performance. *Int J Pharm* 2021;**606**:120893.
40. Sridhar K, Charles AL. *In vitro* antioxidant activity of Kyoho grape extracts in DPPH and ABTS assays: estimation methods for EC_{50} using advanced statistical programs. *Food Chem* 2019;**275**:41−9.

41. Cacua K, Ordoñez F, Zapata C, Herrera B, Pabón E, Buitrago-Sierra R. Surfactant concentration and pH effects on the zeta potential values of alumina nanofluids to inspect stability. *Colloids Surf A* 2019; **583**:123960.
42. Liu Y, Wu C, Hao Y, Xu J, Zhao Y, Qiu Y, et al. Preparation of a novel starch-derived three-dimensional ordered macroporous carbon for improving the dissolution rate and oral bioavailability of water-insoluble drugs. *J Pharm Biomed Anal* 2016;**118**:267−75.
43. Kalepu S, Nekkanti V. Insoluble drug delivery strategies: review of recent advances and business prospects. *Acta Pharm Sin B* 2015;**5**: 442−53.
44. Chen L, Okuda T, Lu XY, Chan HK. Amorphous powders for inhalation drug delivery. *Adv Drug Deliv Rev* 2016;**100**:102−15.
45. Woo MW, Mansouri S, Chen XD. Antisolvent vapor precipitation: the future of pulmonary drug delivery particle production? *Expert Opin Drug Deliv* 2014;**11**:307−11.
46. Yang H, Le QV, Shim G, Oh YK, Shin YK. Molecular engineering of antibodies for site-specific conjugation to lipid polydopamine hybrid nanoparticles. *Acta Pharm Sin B* 2020;**10**:2212−26.
47. McClure R, Ong H, Janve V, Barton S, Zhu M, Li B, et al. Aerosol delivery of curcumin reduced amyloid-beta deposition and improved cognitive performance in a transgenic model of Alzheimer's disease. *J Alzheimers Dis* 2017;**55**:797−811.
48. Taki M, Tagami T, Fukushige K, Ozeki T. Fabrication of nanocomposite particles using a two-solution mixing-type spray nozzle for use in an inhaled curcumin formulation. *Int J Pharm* 2016;**511**:104−10.
49. Adjemian S, Oltean T, Martens S, Wiernicki B, Goossens V, Vanden Berghe T, et al. Ionizing radiation results in a mixture of cellular outcomes including mitotic catastrophe, senescence, methuosis, and iron-dependent cell death. *Cell Death Dis* 2020;**11**:1003.
50. Poinard B, Lam SAE, Neoh KG, Kah JCY. Mucopenetration and biocompatibility of polydopamine surfaces for delivery in an *ex vivo* porcine bladder. *J Control Release* 2019;**300**:161−73.
51. Hu S, Yang Z, Wang S, Wang L, He Q, Tang H, et al. Zwitterionic polydopamine modified nanoparticles as an efficient nanoplatform to overcome both the mucus and epithelial barriers. *Chem Eng J* 2022; **428**:132107.
52. Kiang JG, Olabisi AO. Radiation: a poly-traumatic hit leading to multi-organ injury. *Cell Biosci* 2019;**9**:25.
53. Yu X, Li M, Zhu L, Li J, Zhang G, Fang R, et al. Amifostine-loaded armored dissolving microneedles for long-term prevention of ionizing radiation-induced injury. *Acta Biomater* 2020;**112**:87−100.
54. Li H, Liang X, Duan J, Chen Y, Tian X, Wang J, et al. ROS-responsive EPO nanoparticles ameliorate ionizing radiation-induced hematopoietic injury. *Biomater Sci* 2021;**9**:6474−85.
55. Qin M, Chen W, Cui J, Li W, Liu D, Zhang W. Protective efficacy of inhaled quercetin for radiation pneumonitis. *Exp Ther Med* 2017;**14**: 5773−8.
56. Barnes PJ. Targeting cytokines to treat asthma and chronic obstructive pulmonary disease. *Nat Rev Immunol* 2018;**18**:454−66.
57. Jang SS, Kim HG, Lee JS, Han JM, Park HJ, Huh GJ, et al. Melatonin reduces X-ray radiation-induced lung injury in mice by modulating oxidative stress and cytokine expression. *Int J Radiat Biol* 2013;**89**: 97−105.
58. Lierova A, Jelicova M, Nemcova M, Proksova M, Pejchal J, Zarybnicka L, et al. Cytokines and radiation-induced pulmonary injuries. *J Radiat Res* 2018;**59**:709−53.
59. Wei L, Zhang J, Yang ZL, You H. Extracellular superoxide dismutase increased the therapeutic potential of human mesenchymal stromal cells in radiation pulmonary fibrosis. *Cytotherapy* 2017;**19**:586−602.
60. Rabbani ZN, Anscher MS, Folz RJ, Archer E, Huang H, Chen L, et al. Overexpression of extracellular superoxide dismutase reduces acute radiation induced lung toxicity. *BMC Cancer* 2005;**5**:59.
61. Cao K, Lei X, Liu H, Zhao H, Guo J, Chen Y, et al. Polydatin alleviated radiation-induced lung injury through activation of Sirt3 and inhibition of epithelial−mesenchymal transition. *J Cell Mol Med* 2017;**21**:3264−76.
62. Zhao DY, Qu HJ, Guo JM, Zhao HN, Yang YY, Zhang P, et al. Protective effects of myrtol standardized against radiation-induced lung injury. *Cell Physiol Biochem* 2016;**38**:619−34.
63. Rahi MS, Parekh J, Pednekar P, Parmar G, Abraham S, Nasir S, et al. Radiation-induced lung injury-current perspectives and management. *Clin Pract* 2021;**11**:410−29.
64. Cain DW, Cidlowski JA. Immune regulation by glucocorticoids. *Nat Rev Immunol* 2017;**17**:233−47.
65. Coutinho AE, Chapman KE. The anti-inflammatory and immunosuppressive effects of glucocorticoids, recent developments and mechanistic insights. *Mol Cell Endocrinol* 2011;**335**:2−13.